DNA vaccination for cervical cancer; a novel technology platform of RALA mediated gene delivery via polymeric microneedles.

Ali, A. A., McCrudden, C. M., McCaffrey, J., McBride, J. W., Cole, G., Dunne, N. J., Robson, T., Kissenpfennig, A., Donnelly, R. F., & McCarthy, H. O. (2017). DNA vaccination for cervical cancer; a novel technology platform of RALA mediated gene delivery via polymeric microneedles. *Nanomedicine: Nanotechnology, Biology and Medicine*, *13*(3), 921-932. https://doi.org/10.1016/j.nano.2016.11.019

Published in:
Nanomedicine: Nanotechnology, Biology and Medicine

Document Version:
Peer reviewed version

Queen's University Belfast - Research Portal:
Link to publication record in Queen's University Belfast Research Portal

DNA Vaccination for Cervical Cancer; A Novel Technology Platform of RALA Mediated Gene Delivery via Polymeric Microneedles

Ali AA[1], McCrudden CM[1], McCaffrey J[1], McBride JW[1], Cole G[1], Dunne NJ[2], Robson T[3], Kissenpfennig A[4], Donnelly RF[1], McCarthy HO[1].

[1] School of Pharmacy, Queen's University Belfast, 97 Lisburn Road, Belfast BT9 7BL, UK

[2] School of Mechanical and Manufacturing Engineering, Dublin City University, Dublin 9, Ireland

[3] Molecular & Cellular Therapeutics, Royal College of Surgeons in Ireland

123 St Stephens Green, Dublin 2, Ireland

[4]The Centre for Infection and Immunity, The Wellcome-Wolfson Institute for Experimental Medicine, Queen's University Belfast, Belfast, BT9 7AE, UK

Corresponding Author:

Helen O McCarthy

School of Pharmacy, Queen's University Belfast,

97 Lisburn Road, Belfast, BT9 7BL

UK Phone: +44(0) 28 90972149

Fax +44(0) 28 90247794

Email: h.mccarthy@qub.ac.uk

Abstract word count **(150)**

Manuscript word count (including body text and figure legends **(5000)**

Number of figures **(8)**

Number of references **(50)**

Abstract

HPV subtypes (16, 18) are associated with the development of cervical cancer, with oncoproteins E6 and E7 responsible for pathogenesis. The goal of this study was to evaluate our 'smart system' technology platform for DNA vaccination against cervical cancer. The vaccination platform brings together two main components; a peptide RALA which condenses DNA into cationic nanoparticles (NPs), and a polymeric polyvinylpyrrolidone (PVP) microneedle (MN) patch for cutaneous delivery of the loaded NPs. RALA condensed E6/E7 DNA into NPs not exceeding 100 nm in diameter, and afforded the DNA protection from degradation in PVP. Sera from mice vaccinated with MN/RALA-E6/E7 were richer in E6/E7-specific IgGs, displayed a greater T-cell-mediated TC-1 cytotoxicity and contained more IFN-γ than sera from mice that received NPs intramuscularly. More importantly, MN/RALA-E6/E7 delayed TC-1 tumour initiation in a prophylactic model, and slowed tumour growth in a therapeutic model of vaccination, and was more potent than intramuscular vaccination.

Keywords: DNA vaccination; Microneedles; RALA Peptide; Cervical Cancer

1. Background

Cervical cancer is the second most common cancer in women with 90% of cervical cancers caused by high-risk HPV strains such as types 16 and 18[1]. Recently, two licensed prophylactic HPV vaccines, Gardasil® and Cervarix® have demonstrated efficacy as preventative vaccines[2], that act by producing antibodies against specific HPV serotypes[3]. However, issues include patient compliance and a lack of efficacy against established HPV infections. This is due to the fact that upon infection, the intracellular location of the virus confers resistance to antibody attack[4]. For this reason, the development of a therapeutic HPV vaccine to treat patients with established HPV infections is clearly an unmet need[5].

HPV early proteins, particularly E6 and E7 viral genes are candidate target antigens for therapeutic vaccination; responsible for malignant transformation and tumour growth[6]. The E6 and E7 viral proteins disrupt tumour suppressor functions of p53 and the retinoblastoma protein (pRb) respectively[7]. The E6 protein stimulates p53 degradation via cellular ubiquitination, which disrupts the control of cell cycle progression. While the E7 protein disturbs pRb, repressing regulation of replication-associated genes[8]. Several therapeutic vaccine applications for HPV-16 E6 and E7 have been studied in preclinical models over the past two decades[9-12], with limited success [13].

DNA vaccination has become an effective strategy for the development of therapeutics against many types of cancer, including breast, ovarian, prostate[14], and cervical carcinoma[15]. Numerous DNA vaccines directed against either HPV16 E6 or E7 have been tested with promising results in murine models[16-20]. However, successful implementation of DNA-based vaccination strategies requires a robust gene delivery vehicle capable of penetrating plasma membranes, protecting the nucleic acid cargo from intercellular degradation and ensuring the delivery to the nucleus of the target cell[21]. There is also a need to deliver the DNA to

antigen presenting cells (APCs), so that the intracellular antigens are processed through both the MHC class I and II presentation pathways, ensuring a full complement of cellular and humoral immune responses[22]. We have bioengineered a novel 30 amino acid cationic peptide delivery sequences, termed RALA. RALA consists of arginine/alanine/leucine/alanine repeats, interacts with anionic nucleic acids via electrostatic interaction to form nanoscale cationic particles. Moreover, RALA's hydrophobic and hydrophilic regions facilitate interaction with the lipid bilayers, enabling transport of DNA across cellular membranes, endosomal disruption enabling transport of DNA to the nucleus. We have previously reported RALA's ability to evoke reporter transgene expression *in vitro* and *in vivo*[23-24].

An emerging strategy to intramuscular vaccination is to target the APC population residing in the dermis via different delivery methods such as electroporation, tattooing, or microneedle (MN) arrays. The advantages of MN technology include pain free administration, simplicity of use, lack of needle stick injury, patient compliance and low manufacturing costs[25]. MNs are designed to painlessly breach the skin's *stratum corneum (SC)* barrier and dissolve upon contact with the skin's interstitial fluid to release the cargo in the needle tips[26, 27]. Herein we build upon the delivery of DNA from this system[28] and report for the first time on a functional HPV-16 E6/E7 DNA vaccine candidate. In this investigation RALA-E6/E7 NPs were loaded into soluble MN arrays, and we demonstrate how effective this unique technology platform is compared to injectable systems *in vivo*.

2. Methods

2.1 Preparation of RALA-E6/E7 nanoparticles

The RALA peptide (Biomatik, USA) was supplied as a desalted lyophilized powder, and reconstituted as described previously[23]. DNA encoding the HPV-16 E6 and E7 antigens was purchased from Addgene (USA). The expression vector p1321 vector contained the genes for HPV16 E6, or E7 or E6/E7, the β-actin promoter and an ampicillin selective marker. RALA-E6/E7 NPs were prepared at N:P ratios (the molar ratio of positively charged nitrogen atoms in the peptide to negatively charged phosphates in the pDNA backbone) ranging from 1 to 12 by adding appropriate volumes of peptide solution to 1 μg pDNA. RALA-E6/E7 NPs were incubated at 19°C for 30 min to allow the formation of the NPs.

2.2 DNA neutralisation assay

RALA-E6/E7 at N:P ratios 0.25–12 were electrophoresed through a 1% agarose gel (Life Technologies, UK) with Tris acetate running buffer at 80 V for 60 min, and gels were visualized using a Multispectrum Bioimaging System (UVP, UK).

2.3 Particle size and zeta potential analysis

RALA-E6/E7 NPs were prepared at N:P ratios 2-12. The particle size and zeta potential was measured using a Nano ZS Zetasizer and DTS software (Malvern Instruments, UK) at 25^{o}C. Variations included size from 4-37^{o}C and storage of NPs at RT up to 1 month. Each measurement (n=3) had 15 sub measurements.

2.5 Serum stability study

RALA-E6/E7 NPs were incubated for up to 6 h at 37°C in 10% fetal calf serum. Subsequently, Proteinase K (Sigma-Aldrich, UK) was added (1 mg/ml) to decomplex the pDNA from RALA and samples were electrophoresed.

2.7 Heparin stability study

DNA was labelled with Quant-iT™ PicoGreen® dsDNA reagent (Life Technologies, UK). Heparin sulfate (Sigma, UK) (10–20 U/mL) was added to the NPs and the dissociation

properties of the NPs were measured via fluorescence (FLUOstar OPTIMA; BMG LABTECH, USA) with an excitation wavelength of 480 nm and a detection wavelength of 520 nm.

2.8 Transmission electron microscopy (TEM)

RALA-E6/E7 NPs were prepared at a N:P ratio of 10 and loaded onto a Formvar/Carbon mesh grid (Agar Scientific, UK). The grid was dried overnight and stained for 5 min with 5% aqueous uranyl acetate at 19°C. The grid was imaged using a JEOL 100CXII transmission electron microscope at an accelerating voltage of 80 kV.

2.9 Encapsulation assay

RALA-E6/E7 NPs were prepared and Quant-iT™ PicoGreen® Reagent (Life Technologies, UK) was added to each sample. The percentage encapsulation was calculated relative to naked DNA controls. Sample fluorescence was analyzed as per 2.7.

2.10 *In vitro* transfections

NCTC-929 fibroblast cells (ATCC) were seeded, conditioned for 2 h in Opti-MEM (Gibco, UK), which was then supplemented with 50 µl RALA/pDNA NPs. For comparison, cells were also transfected with Lipofectamine 2000 or polyethylenimine (PEI) (Life Technologies, UK). After 6 h the media was removed and replaced with serum-supplemented culture medium.

2.11 Western blot analysis

NCTC-929 cell lysates were collected with radio immune precipitation assay (RIPA) buffer to determine the level of HPV-16 E6 and HVP-16 E7 protein expression. Each sample (20 µg) was electrophoresed through a 4-12% sodium dodecyl (SDS)-polyacrylamide gel (Life Technologies, UK), transferred onto a nitrocellulose membrane (Hybond-C, Amersham; UK) and probed with HPV-16 E6 and HVP-16 E7 antibodies (Abcam; UK). GAPDH was used as a loading control (Sigma; UK). Levels of protein expression were assessed using an Immobilon western detection kit (Millipore; UK). X-ray films were scanned using benchtop UV transilluminators (UVP Products Ltd) and density was calculated using Image J (http://rsbweb.nih.gov/ij/) incorporating correction of loading controls.

2.12 Fabrication of polymeric MN arrays

RALA-E6/E7 loaded MNs were prepared using the micro-moulding process illustrated in Fig. 4a. A 40% stock solution of PVP (360 kDa) (Sigma; UK) was prepared 50:50 with NP solution. 25 mg of the polymeric gel containing the NPs was weighed into the moulds and centrifuged to ensure the MN cavities were filled. A further 0.5 g of 20% PVP polymer was added to the moulds to form the baseplate to which the MNs are attached and centrifuged again. The arrays were left to dry at room temperature, and after 48 h, were manually released from the moulds and the polymeric sidewalls removed using a heated scalpel. Each MN array contained 361 (19x19) needles 600 μm high with base width of 300 μm and 300 μm interspacing.

2.13 Measurement of MN height reduction

To determine the axial force required for mechanical fracture of the MNs, the TA-XT2 texture analyser (Stable Microsystems, UK) was employed. MN arrays were attached to the moveable cylindrical probe of the texture analyser. An axial compression load of 45 N was applied to the polymeric MN arrays[29]. The height of the MNs was measured using a digital microscope (GE-5 USB) at 180x magnification.

2.14 Optical coherence tomography (OCT)

Neonatal full thickness porcine skin was prepared and equilibrated in PBS for 30 min at 37°C to restore conditions resembling the *in vivo* state. The skin was then placed onto a sheet of dental wax for support with the SC side facing towards the environment. Manual application using the thumb for 30 sec was applied. Images were taken every 5 min to monitor the MNs dissolution profile. Depth of insertion of the MNs into the skin was determined using Image J software.

2.15 Measurement of MN Stability

The MN/RALA-E6/E7 vaccine was packed in air tight packing film in temperature controlled environments of 4.0 ± 1.0 °C, RT (20.0 ± 1.0 °C), and 37 ± 1.0 °C. After 28 days, MNs were dissolved in OptiMEM serum free media for 2 h and NCTC-929 cells were transfected (2.16).

2.16 Cell viability analysis

NCTC-929 cells were seeded for 24 h prior to the assay. Media were supplemented with 5, 10 or 20 mg/mL of 20% polymer (PVP) and incubated for 24 h. 10% MTS reagent (Promega, UK) was added to the cell medium and incubated for a further 2 h. Absorbance was measured at 450 nm on an EL808 96-well plate reader (BioTek Instruments Inc, UK).

2.17 Clonogenic Assay

24 h post transfection, NCTC-929 cells were plated at a density of 200 and 500 cells per well. Plates were then incubated for 14 days at 37^{o}C in 5% CO_2/95% air and then colonies were fixed and stained with 0.4% crystal violet in 70% methanol and counted manually.

2.18 Quantification of DNA cargo delivered *in vivo*

NP-loaded MNs were applied to the dorsal surface of C57BL/6 mice ears (Charles River, UK) for 5 min, followed by removal of the array and quantification of the DNA remaining in the array using Quant-iT™ PicoGreen® dsDNA reagent (Life Technologies, UK). The remaining array was dissolved in 5 mL Tris buffer (10 mM) for 1 h and 50 µL of 1 mg/mL Proteinase K was subsequently added and samples incubated at 37°C for 1 h. Sample fluorescence was analyzed as per 2.7.

2.19 Immunization of mice

The experimental protocols were compliant with the UK Scientific Act of 1986, project license 2794 and were approved by QUB ethics committee. C57BL/6 mice were immunized with approximately 50 µg of either naked DNA (HPV-16 E6E7) or RALA-E6/E7 NPs by either I.M. or MN application on mice ears. Vaccination was followed by a 2nd and 3rd booster immunizations every 2 weeks. MN arrays laden with NPs or DNA were manually inserted

onto the dorsal side of both ears. The MNs were held in place for at least 5 min, secured in place using surgical adhesive tape, and then removed 24 h following application.

2.20 ELISA for detecting anti-E6/E7 antibodies

An indirect ELISA was carried out after the 2nd and 3rd boosts to determine E6/E7 specific IgG antibodies in mice sera. A 96 well plate was coated with 100 µl of purified HPV-16 E7/E6 peptides (Proimmune, UK) at 0.5 mg/ml and incubated at 4°C overnight. After washing the serum samples diluted in PBS (1:100) were added to the ELISA wells. The plate was incubated with a 1:2000 dilution of a goat anti-mouse IgG HRP-conjugated antibody (Sigma, UK) at RT for 1 h. An enzyme substrate (OPD, Sigma) was added for colour development and Immunoreactivity was detected with an ELISA plate reader at 450 nm. Quantification of IgG was performed using an Easy Titer IgG assay kit (Thermo scientific, UK).

2.21 Cytotoxicity Assay

Following the third immunization, the spleen from each mouse was aseptically removed, homogenized and re-suspended in RBC lysis buffer (Sigma, UK). T cells (used as the effecter cells) were co-cultured at a ratio of 10:1 with irradiated TC-1 cells (10^4 per well) (used as the target cells) in RPMI-1640 medium with 20 units of interleukin-2 (Peprotech, UK) in 24-well plates (Corning) at 37°C for 6 days. The TC-1 cells were kindly provided by Dr Wu (Johns Hopkins University). *In vitro* radiation experiments were performed using a 160 kVp x-ray source (Faxitron X-ray, USA) with a 0.8 mm filter. Viable T cells were seeded with non-irradiated TC-1 cells in the ratios of 5:1 and 10:1, respectively, in an assay medium (1% BSA medium) in triplicate at 37°C for 5 h in 96-well plates. After 5 h, the supernatant of each sample was collected and TC-1 cytotoxicity was measured using a LDH cytotoxicity detection kit (Roche, UK).

2.22 Interferon-ɣ assay

After the third immunization, spleens were removed and T cells (used as the effecter cells) were co-cultured at a ratio of 10:1 with irradiated TC-1 cells (10^4 per well) (used as the

target cells), with 20 units of interleukin-2 (Peprotech, UK) in 24-well plates (Corning) at 37°C for 4 days. The supernatant (100 µl) of each sample was taken after removing any debris by centrifugation. Interferon-ɣ was detected using Interferon-ɣ ELISA kit (Peprotech, UK).

2.23 Tumour prophylactic assay

C57BL/6 mice (n=9 per group) were immunized as 2.19. One week after the last vaccination, mice were challenged with $1X10^5$ TC-1 cells/mouse in PBS implanted i.d. on the rear dorsum. The mice were monitored for evidence of tumour growth by palpation and measurement three times a week.

2.24 Tumour challenge assay

C57BL/6 mice (n=9 per group) were injected i.d. on the rear dorsum with $1X10^5$ TC-1 cells/mouse. When tumours reached 50 mm^3, mice were immunized with either 100 µg naked DNA (HPV-16 E6E7) or RALA-E6/E7 NPs by either I.M. or MN application on the ears. Vaccination was followed by 2^{nd} and 3^{rd} booster immunizations every 2 weeks. Tumour dimensions were measured three times per week. In both *in vivo* studies, tumour volume was calculated using the formula

$$V = \frac{4}{3}\pi r^3$$

Where r is half of the geometric mean diameter (GMD), calculated as

$$\sqrt[3]{L*B*D}$$

2.25 Statistical analysis

All experiments has at least three independent replicates, and results are expressed as mean ± standard error (SE). Significance of differences was calculated using the two-tailed

unpaired t-test with a p value of ≤ 0.05 considered significant. Statistical analyses of the survival curves were calculated using the log rank (Mantel-Cox) test with a p value of ≤ 0.05 considered significant. Statistical analyses were performed using Prism 5.0 (GraphPad Software; CA).

3. Results

3.1 Characterization and stability of RALA-E6/E7 NPs

Results indicated that the RALA-E6/E7 NPs were formed from N:P 1 onwards; RALA prevented electrophoretic migration of DNA through the gel (Fig. 1a). RALA-E6/E7 NPs had an average hydrodynamic size of approximately 61.8-99.5 nm across all N:P ratios with a polydispersity index (PDI) <0.4 indicating a relatively homogenous population. The zeta-potential of the RALA-E6/E7 NPs was 20-30 mV from N:P 4 upwards (Fig. 1b). TEM imaging at N:P 10 also revealed a core radius of NPs of approximately 70.9 nm (Fig. 1c). Encapsulation values of >90% from N:P 4 upwards indicated efficient complexation (Fig. 1d).

RALA-E6/E7 NPs remained stable at room temperature for up to 30 days and also over a range of temperatures (4-37^{o}C) (Fig. 2a & b). Further investigations revealed that RALA preserved the integrity of the E6/E7 DNA in the presence of serum and after exposure to heparin (Fig. 2c & d). This confirms that the NPs could remain intact in the presence of simulated biological fluids.

3.2 In vitro gene expression with RALA-E6/E7 NPs

RALA-E6/E7 NPs successfully transfected NCTC-929 cells as demonstrated by over expression of both HPV-16 E6 and HPV-16 E7 antigens compared to untreated cells (Fig. 3a). Toxicity of RALA is considerably reduced at 8.9% compared to commercially available agents such as Lipofectamine 2000 (25.6%) and PEI (70%) (Fig. 3b).

3.3 The RALA-E6/E7 NPs do not compromise the PVP matrix

A single MN array contains 361 projections (Fig. 4a), resulting in approximately 5 mg of 20% PVP. Results indicated that 20% PVP caused no significant cellular toxicity. Following exposure to the highest concentration (20 mg/mL) of PVP for 24 h, the % cell viability was 87.5% compared to untreated cells ($p= 0.1597$, using a one-tailed, unpaired t-test). Morphologically, 20 mg/ml-treated cells did not appear to differ from control cells (Fig. 4b).

Axial fracture force tests determined the mechanical strength of the PVP polymeric MNs. Using manual force, a penetration depth of 90% of needle length was achieved, and the needles were not broken or deformed by the process (Fig. 4c). Importantly, MNs that were loaded with RALA/E6-E7 NPs were still able to penetrate the skin effectively, displaying similar insertion mechanics to 'empty' MNs (20% PVP only). Furthermore, after evaluation of *in situ* dissolution kinetics of the MNs, it was found that by 15 min, MNs had both lost their needle profile and efficiently dissolved within the skin layers (Fig. 4c). Further analysis of E6/E7 (DNA only) or RALA-E6/E7 NP-loaded MN array revealed that an application of 45 N force to MN tips resulted in modest 10.2% and 9.2% reduction in needle height respectively, which was not significantly different from empty MNs with 10.8% reduction in needle height ($p= 0.7775$ & 0.4150 for DNA and RALA/E6-E7 NPs loaded MNs compared to empty MNs).

3.4 RALA-E6/E7 NP release and functionality following incorporation in PVP matrix

NCTC-929 cells transfected with RALA-E6/E7 NPs liberated from the PVP MN matrix expressed the viral proteins, yet naked E6/E7 DNA released from the PVP matrix was unable to evoke protein expression (Fig. 5a) indicating that RALA is necessary for the functionality of the E6/E7 DNA within the PVP matrix. Furthermore, PVP did not compromise functionality of the NPs after 28 days storage with a significant increase in HPV-16 E6/E7 protein expression compared to untreated cells (Fig 5b).

For release experiments *in vivo*, MN arrays were fabricated to contain 36 μg total DNA; however not the entire DNA will be present in the final MN array. Of the 36 μg total DNA initially incorporated into MN arrays, 30.2 ± 1.29 μg could be detected upon re-dissolution of the arrays; of that, 20.7 μg was present in the arrays following removal of excess sidewalls. For this reason, we therefore determined 20.7 μg to be deliverable using our MN array. Following a 5 min application to mouse ears, MN arrays were found to retain 9.5 μg DNA, indicating that 11.4 μg had been delivered; additionally, following a 24 h application procedure, only 1.9 μg DNA was retained in the arrays, indicating that 91% of the was delivered during a 24 h application (Fig. 5b).

3.5 MN/RALA-E6/E7 evokes a consistent humoral and cell-mediated immune response

Following immunization (Fig. 6a), it was shown that the concentration of antibodies from the NP groups (either I.M. or MN) was 2x that of the control group (Fig. 6b). These results suggest DNA vaccination using our MN-NP system elicits a robust antigen-specific humoral immune response, facilitating immunogenic memory at levels comparable, and even superior, to those observed following I.M. injections.

Cytotoxicity and interferon-γ assays were carried out to test the immune response generated by the killing of the HPV-16 oncogenic antigen expressing cells (TC-1) by the E6/E7 plasmid. MN/RALA-E6/E7-vaccinated mice evoked a two-fold higher TC-1 cytotoxicity than control mice. Additionally the cytotoxicity was greater in MN/RALA-E6/E7-vaccinated mice than in any other treatment group (Fig. 7a), indicating a robust immune response from MN/RALA-E6/E7 immunization.

The IFN-γ release assay demonstrates that when primed T cell-enriched splenocytes were cultured without TC-1 cells, the amount of interferon-γ secreted was almost undetectable (Fig. 7b). However, when the primed T cell-enriched splenocytes were co-cultured with TC-1 cells, there was an increase in the amount of IFN-γ released by the T cell-enriched splenocytes; the most impressive release of IFN-γ was from the MN/RALA-E6/E7-vaccinated

mice, which was significantly higher than the degree of IFN-γ released by T cells from naïve mice (p= 0.035 for mice vaccinated with MN/RALA-E6/E7 compared to controls). This is indicative of a cytotoxic T cell-mediated immune response.

3.6 MN/RALA-E6/E7 vaccination prevents the uptake of tumours and slows the growth of established tumours

In the prophylactic study, tumours were palpable at seven days post-challenge (i.d.) in controls, however vaccinated groups remained tumour-free up to 10 days, with tumours undetectable in the MN/RALA-E6/E7 group until 16 days. At day 20 post-challenge, the GMD of the tumours of all control mice and the empty MN group reached the pre-determined ethical study endpoint. Furthermore the growth of the tumours in the MN/RALA-E6/E7 was significantly retarded compared to the controls (p= 0.002 using two-tailed unpaired t-test). Figure 8a shows that that 4 out of 9 (44%) mice challenged did not develop any tumours after vaccination with MN/RALA-E6/E7. Immunization with RALA-E6/E7 NPs via the I.M. route also completely inhibited tumour development in 2 out of 9 mice (22.2%), while naked DNA (HPV-16 E6E7) delivered either by I.M. or MN application showed lower survival (only 1 out 9 mice survived).

In the therapeutic arm of the study, we determined that MN/RALA-E6/E7 vaccination of mice with pre-existing tumours caused complete regression of tumours in 2/9 mice *(2 mice were censored because of other causes but their GMDs were < 12 mm)*. Whereas when mice were vaccinated using RALA-E6/E7 by the I.M. route or naked DNA in MN, complete regression was observed in only 11% of mice (1/9). None of the other vaccination strategies significantly altered tumour growth kinetics/mouse survival (Fig. 8b). Furthermore, a clear difference in the tumour volume was found for the tumour-bearing mice that followed MN/RALA-E6/E7 vs other vaccination strategies (p= 0.004 two-tailed unpaired t-test). For example, after 20 days, the mean tumour volume for mice vaccinated with MN/RALA-E6/E7

was 246 mm^2 compared to 486.85, 503.13, and 633.2 mm^2 for mice vaccinated with MN/E6/E7, RALA-E6/E7 I.M, and E6/E7 I.M respectively.

4. Discussion

In this study, we validated a new system for the delivery of a HPV DNA therapeutic vaccine, which overcomes both intracellular and extracellular barriers using RALA/E6-E7 NPs, loaded in a PVP-based MN platform. Immune responses can be augmented by utilising delivery systems to protect the DNA cargo and facilitate delivery to APCs[30]. For optimal cell uptake, NPs should be less than 150 nm in diameter, have sufficient cationic charge to prevent aggregation in order to bind to the negatively charged cell membrane[23]. In this study, RALA conferred ideal size and charge characteristics on the E6-E7 DNA to facilitate efficient cellular uptake and antigen expression.

The increased incidence of APCs in the dermal region has garnered interest in transcutaneous DNA vaccine delivery. Lower numbers of APCs are associated with I.M. vaccination and so efficient drainage to lymph nodes is required for antigen presentation[31]. A number of *in vivo* studies have demonstrated that MN immunization elicits an efficient immune response[32, 33]. Naked DNA[34], influenza[35] and HPV virus-like particles (VLP) [36], have elicited both B- and T-cell immune responses after administration to the skin using MNs. Rapid dissolution of MN arrays in the skin could be advantageous for vaccination and PVP can be safely excreted through the kidneys within a few days[32,37]. In this study the MNs could penetrate skin effectively and more importantly, MN-NP arrays retained functionality following extended storage conditions. Results revealed efficient transfection with RALA/E6-E7 NPs with no transfection with naked HPV-16 E6-E7 into the polymer suggesting that the RALA is essential to protect the DNA in polymeric MN system. Similar observations have been reported where poly(lactic-co-glycolic acid) (PLGA) dissolving MNs adversely affected the stability of naked pDNA, with a subsequent loss of bioactivity [38].

It has been reported that a low dose of HPV16 PsV-encapsidated DNA (0.3 μg) incorporated into MNs effectively produced neutralizing antibody response against HPV[39]. Therefore, the quantity of DNA (10 μg) that we can deliver via the ear pinna should be sufficient to evoke an immune response. The ear pinna exhibits two layers of epidermis and dermis, separated by cartilage, thereby doubling the amount of professional APCs, which after appropriate activation, migrate to one major pinna draining lymph node, eliciting rapid immune response induction[40]. Indeed humoral and cytotoxic T cell-mediated immune responses after intra ear pinna (i.e.) DNA vaccination have been ~10 times stronger than I.M. immunizations[40, 41]. Typical target cells include keratinocytes, Langerhans' cells, and dermal dendritic cells (DCs). Once mature, DCs can migrate to local lymph nodes where antigens are presented to T cells and the initiation of a variety of immunological responses ensues. In our immune analysis, the best humoral immune responses were obtained with MN/RALA-E6/E7 group where a titer of 50 μg/ml was induced after 5 weeks and sustained following 8 weeks of immunization. Although humoral responses are unlikely to mediate cervical cancer regression or elimination of infection directly, these responses do affirm the immunogenicity of MN/RALA-E6/E7-vaccine. The significant increase of HPV16 E6 and E7-specific T cell immunity was identified via cytotoxicity and interferon γ ELISA assay after vaccination. MN/RALA-E6/E7-vaccinated mice evoked a two-fold higher TC-1 cytotoxicity than control mice, and a significant target-cell lysis was observed even at low effector-to-target ratios. Primed T cells can respond quickly and strongly when they come in contact with antigens previously encountered, leading to large amount of interferon-γ secretion[42]. A significant release of interferon γ from MN/RALA-E6/E7 vaccinated mice confirmed the cytotoxic T cell-mediated immune response, which suggests that MN/RALA-E6/E7 elicited antigen-specific cell mediated immune responses superior to those observed by I.M. injections.

Furthermore the MN/RALA-E6/E7 vaccine generated a potent prophylactic antitumor effect against cervical tumour development. In a therapeutic regimen MN/RALA-E6/E7 elicited both a reduction in tumour size and prolonged survival. MN administration of the NPs induced a greater anti-tumour effect than the i.m. route which could be attributed to targeting more APCs within the skin. Activation and subsequent maturation of APCs will induce CD+8 killer lymphocytes and tumour infiltration. Indeed, previous studies have shown that MN vaccination rapidly induces specific tumour infiltrating CD8+ T cells [43-44]. In both arms of the study, administration of E6/E7 peptides had no effect on tumour survival. Poor immunogenicity of peptide-based vaccines is not uncommon as they are heavily affected by the restriction of MHC[45]. However it is also recognized that DNA vaccines can have limited immunogenicity in animal models[46]. Therefore future studies could focus on the co-administration of adjuvants, such as the C-terminal fragment of glycoprotein 96 (gp96), to stimulate E7- specific immune responses[47]. The further advantage of our nano-technology is that a bi or trivalent strategy can be incorporated into the MN patch.

In this study, we have demonstrated successful cutaneous delivery of a DNA vaccine via *in vivo* delivery of NPs, resulting in a robust antigen-specific immune response. Furthermore, prophylactic vaccination using NP-loaded MNs protected against cervical tumour development, and delayed the progression of established cervical cancer xenografts. Such MN-based DNA vaccines do not require cold-chain storage thus reducing costs, and ultimately should improve patient compliance. The licensing of four DNA vaccines in the veterinary medicine field[48] provides optimism that DNA vaccines may soon be approved for applications in humans[49,50], and this study should represent an important breakthrough technology for antigen-associated cancers.

5. Figure Legends

Fig. 1: Physiochemical Characterization of the RALA-E6/E7 NPs. A) Gel retardation assay of RALA-E6/E7 NPs over a range of N:P ratios (0-12). B) Particle size, zeta potential and polydispersity index of RALA-E6/E7 NPs at N:P ratios 2-12. C) TEM image of RALA-E6/E7 NPs N:P ratio of 10. D) Encapsulation assay of RALA-E6/E7 NPs at N:P ratios 2-12. (N= 3 ± SEM)

Fig. 2: RALA-E6/E7 forms stable NPs. A) Size, zeta potential and polydispersity index of RALA-E6/E7 nanoparticles (N:P ratio 10) incubated at 19°C for up to 30 days. B) RALA-E6/E7 nanoparticles are stable over a temperature range (4-37°C). C) Serum stability of RALA-E6/E7 nanoparticles (N:P ratio 10) incubated in water 10% serum at 37˚C and decomplexed with Proteinase K. D) Heparin stability study. (N= 3 ± SEM)

Fig. 3: RALA successfully delivers the therapeutic DNA that encodes HPV-16 E6, HPV-16 E7, or HPV-16 E6/E7. A) E6/E7 protein expression in NCTC-929 fibroblast cells with RALA-E6/E7 nanoparticles for 24 h. B) Clonogenic cell survival. (N= 3 ± SEM)

Fig. 4: RALA-E6/E7 MNs are mechanically strong and biocompatible with PVP matrix. a) Manufacture of the MN-RALA-E6/E7 vaccine patch. B) Cell viability of NCTC-929 fibroblast cells following 24 h exposure to PVP *in vitro.* C) OCT Image of the *in vivo* dissolution profile of MNs laden with RALA-E6/E7 NPs in porcine skin over a 15 min period; dashed line represents the level of the epidermis. Image is representative of 3 separate experiments. D) Percentage height reduction of PVP MN arrays with either no cargo, or loaded with either HPV-16 DNA or NPs. (N=3, mean ± SEM)

Fig. 5: RALA is essential for effective E6/E7 delivery from the optimal MNs. A) Functionality of RALA-E6/E7 following release from 20% PVP MNs. After 24 h samples were analyzed for protein expression by western blot. B) Quantification of HPV-16 E6/E7 DNA in MN arrays 5 min and 24 h post application to C57BL/6 mouse ears. RALA-E6/E7-loaded MN arrays were formulated to contain 36 μg DNA. (N= 3 ± SEM)

Fig. 6: MN-RALA-E6/E7 evokes a consistent humoral mediated immune response. A) Schematic representation of the MN-RALA-E6/E7 vaccine regimen. B) Detection of E6/E7 specific IgG levels following 2^{nd} and 3^{rd} booster immunizations in C57BL/6 mice *in vivo.* Following each immunization, blood serum was isolated and IgG levels measured via ELISA. (N=4 ± SEM).

Fig. 7: MN-RALA-E6/E7 produces cell-mediated immune response. A) The cytotoxicity of T cells against TC-1 cells. 5:1 and 10:1 ratios indicates the different ratios of the effector cells (T cells) to the target cells (TC-1). T cells obtained from treatment groups were cultured with irradiated TC-1 cells for 6 days, and were subsequently purified and incubated with healthy TC- 1 cells for 5 h. B) INF γ levels following 3 immunizations with the MN-RALA-E6/E7. Spleens from the mice were removed, T-cells isolated and co-cultured with irradiated TC-1 for 4 days. Supernatants were collected and INF γ levels detected via a sandwich ELISA. (N=3 ± SEM)

Fig. 8: MN-RALA-E6/E7 vaccination prevents the uptake of TC-1 tumours, and delays the progression of established tumours. A) Prophylactic Study - Mice underwent a prime-boost-boost regimen before challenge with $1x10^5$ TC-1 E6/E7-expressing tumour cells implanted intradermally on the rear dorsum (N=9). B) Therapeutic study – $1x10^5$ TC-1 tumour cells were implanted intradermally on the rear dorsum of C57BL/6 mice. Once tumours reached

50 mm^3, a prime-boost-boost vaccine regimen was implemented. Black arrows indicate the time of immunization.

6. Acknowledgements

This research was supported by an Invest Northern Ireland Proof of Concept Grant (PoC330).

7. References

1. Roden R, Wu T. How will HPV vaccines affect cervical cancer? Nature Reviews Cancer 2006;6(10):753-63.
2. Kwak K, Yemelyanova A, Roden RB. Prevention of cancer by prophylactic human papillomavirus vaccines. Curr.Opin.Immunol. 2011;23(2):244-51.
3. Dauner JG, Pan Y, Hildesheim A, Harro C, Pinto LA. Characterization of the HPV-specific memory B cell and systemic antibody responses in women receiving an unadjuvanted HPV16 L1 VLP vaccine. Vaccine 2010;28(33):5407-13.
4. Griesser H, Sander H, Walczak C, Hilfrich RA. HPV vaccine protein L1 predicts disease outcome of high-risk HPV+ early squamous dysplastic lesions. Am.J.Clin.Pathol. 2009 Dec;132(6):840-860.
5. Hung C, Ma B, Monie A, Tsen S, Wu T. Therapeutic human papillomavirus vaccines: current clinical trials and future directions. 2008.
6. Bosch FX, Lorincz A, Munoz N, Meijer CJ, Shah KV. The causal relation between human papillomavirus and cervical cancer. J.Clin.Pathol. 2002 Apr;55(4):244-65.
7. Munger K, Baldwin A, Edwards KM, Hayakawa H, Nguyen CL, Owens M, et al. Mechanisms of human papillomavirus-induced oncogenesis. J.Virol. 2004 Nov;78(21):11451-60.

8. Gan L, Jia R, Zhou L, Guo J, Fan M. Fusion of CTLA-4 with HPV16 E7 and E6 enhanced the potency of therapeutic HPV DNA vaccine. 2014.
9. Frazer IH, Leggatt GR, Mattarollo SR. Prevention and treatment of papillomavirus-related cancers through immunization. Annu.Rev.Immunol. 2011;29:111-38.
10. Schiller JT, Müller M. Next generation prophylactic human papillomavirus vaccines. The Lancet Oncology 2015;16(5):e217-25.
11. Brinkman JA, Hughes SH, Stone P, Caffrey AS, Muderspach LI, Roman LD, et al. Therapeutic vaccination for HPV induced cervical cancers. Dis.Markers 2007;23(4):337-52.
12. Albers AE, Kaufmann AM. Therapeutic human papillomavirus vaccination. Public.Health.Genomics 2009;12(5-6):331-42.
13. Kenter GG, Welters MJ, Valentijn ARP, Lowik MJ, Berends-van der Meer, Dorien MA, Vloon AP, et al. Vaccination against HPV-16 oncoproteins for vulvar intraepithelial neoplasia. N.Engl.J.Med. 2009;361(19):1838-47.
14. Senovilla L, Vacchelli E, Garcia P, Eggermont A, Fridman WH, Galon J, et al. Trial watch: DNA vaccines for cancer therapy. Oncoimmunology 2013;2(4):e23803.
15. Morrow MP, Yan J, Sardesai NY. Human papillomavirus therapeutic vaccines: targeting viral antigens as immunotherapy for precancerous disease and cancer. 2013.
16. Hung CF, Monie A, Alvarez RD, Wu TC. DNA vaccines for cervical cancer: from bench to bedside. Exp.Mol.Med. 2007 Dec 31;39(6):679-89.
17. Michel N, Osen W, Gissmann L, Schumacher TN, Zentgraf H, Müller M. Enhanced immunogenicity of HPV 16 E7 fusion proteins in DNA vaccination. Virology 2002;294(1):47-59.

18. Bloy N, Buqué A, Aranda F, Castoldi F, Eggermont A, Cremer I, et al. Trial Watch: Naked and vectored DNA-based anticancer vaccines. OncoImmunology 2015(just-accepted):00-.
19. Tahamtan A, Ghaemi A, Gorji A, Kalhor HR, Sajadian A, Tabarraei A, et al. Antitumor effect of therapeutic HPV DNA vaccines with chitosan-based nanodelivery systems. J.Biomed.Sci. 2014;21(1):1-10.
20. Yang B, Yang A, Peng S, Pang X, Roden RB, Wu T, et al. Co-administration with DNA encoding papillomavirus capsid proteins enhances the antitumor effects generated by therapeutic HPV DNA vaccination. Cell & bioscience 2015;5(1):1-10.
21. Cole G, McCaffrey J, Ali AA, McCarthy HO. DNA vaccination for prostate cancer: key concepts and considerations. Cancer nanotechnology 2015;6(1):1-23.
22. Yewdell JW. Designing CD8 T cell vaccines: it's not rocket science (yet). Curr.Opin.Immunol. 2010;22(3):402-10.
23. McCarthy HO, McCaffrey J, McCrudden CM, Zholobenko A, Ali AA, McBride JW, et al. Development and characterization of self-assembling nanoparticles using a bio-inspired amphipathic peptide for gene delivery. J.Controlled Release 2014;189:141-9.
24. Bennett R, Yakkundi A, McKeen HD, McClements L, McKeogh TJ, McCrudden CM, et al. RALA-mediated delivery of FKBPL nucleic acid therapeutics. Nanomedicine 2015;10(19):2989-3001.
25. McCaffrey J, Donnelly RF, McCarthy HO. Microneedles: an innovative platform for gene delivery. Drug Delivery and Translational Research 2015;5(4):424-37.
26. Quinn HL, Kearney M, Courtenay AJ, McCrudden MT, Donnelly RF. The role of microneedles for drug and vaccine delivery. Expert opinion on drug delivery 2014;11(11):1769-80.

27. McCrudden MT, Torrisi BM, Al-Zahrani S, McCrudden CM, Zaric M, Scott CJ, et al. Laser-engineered dissolving microneedle arrays for protein delivery: potential for enhanced intradermal vaccination. J.Pharm.Pharmacol. 2015;67(3):409-25.
28. McCaffrey J, McCrudden CM, Ali AA, Massey AS, McBride JW, McCrudden MT, et al. Transcending epithelial and intracellular biological barriers; A prototype DNA Delivery device. J.Controlled Release 2016.
29. Larrañeta E, Moore J, Vicente-Pérez EM, González-Vázquez P, Lutton R, Woolfson AD, et al. A proposed model membrane and test method for microneedle insertion studies. Int.J.Pharm. 2014;472(1):65-73.
30. Shah MAA, He N, Li Z, Ali Z, Zhang L. Nanoparticles for DNA vaccine delivery. Journal of biomedical nanotechnology 2014;10(9):2332-49.
31. Marshall S, Sahm LJ, Moore AC. The success of microneedle-mediated vaccine delivery into skin. Human vaccines & immunotherapeutics 2016(just-accepted):00-.
32. Sullivan SP, Murthy N, Prausnitz MR. Minimally invasive protein delivery with rapidly dissolving polymer microneedles. Adv Mater 2008;20(5):933-8.
33. van der Maaden K, Varypataki EM, Romeijn S, Ossendorp F, Jiskoot W, Bouwstra J. Ovalbumin-coated pH-sensitive microneedle arrays effectively induce ovalbumin-specific antibody and T-cell responses in mice. European Journal of Pharmaceutics and Biopharmaceutics 2014;88(2):310-5.
34. Pearton M, Saller V, Coulman SA, Gateley C, Anstey AV, Zarnitsyn V, et al. Microneedle delivery of plasmid DNA to living human skin: formulation coating, skin insertion and gene expression. J.Controlled Release 2012;160(3):561-9.
35. Sullivan SP, Koutsonanos DG, del Pilar Martin M, Lee JW, Zarnitsyn V, Choi S, et al. Dissolving polymer microneedle patches for influenza vaccination. Nat.Med. 2010;16(8):915-20.

36. Corbett HJ, Fernando G, Chen X, Frazer IH, Kendall M. Skin vaccination against cervical cancer associated human papillomavirus with a novel micro-projection array in a mouse model. PLoS One 2010;5(10):e13460.
37. Marin E, Briceno MI, Caballero-George C. Critical evaluation of biodegradable polymers used in nanodrugs. Int.J.Nanomedicine 2013;8:3071-90.
38. Ramgopal Y, Mondal D, Venkatraman S, Godbey W. Sustained release of complexed and naked DNA from polymer films. Journal of Biomedical Materials Research Part B: Applied Biomaterials 2008;85(2):496-503.
39. Kines RC, Zarnitsyn V, Johnson TR, Pang YY, Corbett KS, Nicewonger JD, et al. Vaccination with human papillomavirus pseudovirus-encapsidated plasmids targeted to skin using microneedles. PLoS One 2015 Mar 18;10(3):e0120797.
40. Förg P, Von Hoegen P, Dalemans W, Schirrmacher V. Superiority of the ear pinna over muscle tissue as site for DNA vaccination. Gene Ther. 1998;5(6):789-97.
41. Schirrmacher V, Förg P, Dalemans W, Chlichlia K, Zeng Y, Fournier P, et al. Intra-pinna anti-tumor vaccination with self-replicating infectious RNA or with DNA encoding a model tumor antigen and a cytokine. Gene Ther. 2000;7(13):1137-47.
42. Cheung Y, Cheng SC, Sin FW, Xie Y. Plasmid encoding papillomavirus Type 16 (HPV16) DNA constructed with codon optimization improved the immunogenicity against HPV infection. Vaccine 2004;23(5):629-38.
43. Zaric M, Lyubomska O, Touzelet O, Poux C, Al-Zahrani S, Fay F, et al. Skin dendritic cell targeting via microneedle arrays laden with antigen-encapsulated poly-D, L-lactide-co-glycolide nanoparticles induces efficient antitumor and antiviral immune responses. ACS nano 2013;7(3):2042-55.

44. Hu Y, Xu B, Xu J, Shou D, Liu E, Gao J, et al. Microneedle-assisted dendritic cell-targeted nanoparticles for transcutaneous DNA immunization. Polymer Chemistry 2015;6(3):373-9.

45. Sharma RK, Elpek KG, Yolcu ES, Schabowsky RH, Zhao H, Bandura-Morgan L, et al. Costimulation as a platform for the development of vaccines: a peptide-based vaccine containing a novel form of 4-1BB ligand eradicates established tumors. Cancer Res. 2009 May 15;69(10):4319-26.

46. Kardani K, Bolhassani A, Shahbazi S. Prime-boost vaccine strategy against viral infections: Mechanisms and benefits. Vaccine 2016;34(4):413-23.

47. Bolhassani A, Zahedifard F, Taghikhani M, Rafati S. Enhanced immunogenicity of HPV16E7 accompanied by Gp96 as an adjuvant in two vaccination strategies. Vaccine 2008;26(26):3362-70.

48. Wahren B, Liu MA. DNA vaccines: Recent developments and the future. Vaccines 2014;2(4):785-96.

49. Lu S. Immunogenicity of DNA vaccines in humans: it takes two to tango. Human vaccines 2008;4(6):449-52.

50. Kutzler MA, Weiner DB. DNA vaccines: ready for prime time? Nature Reviews Genetics 2008;9(10):776-88

Figure 1

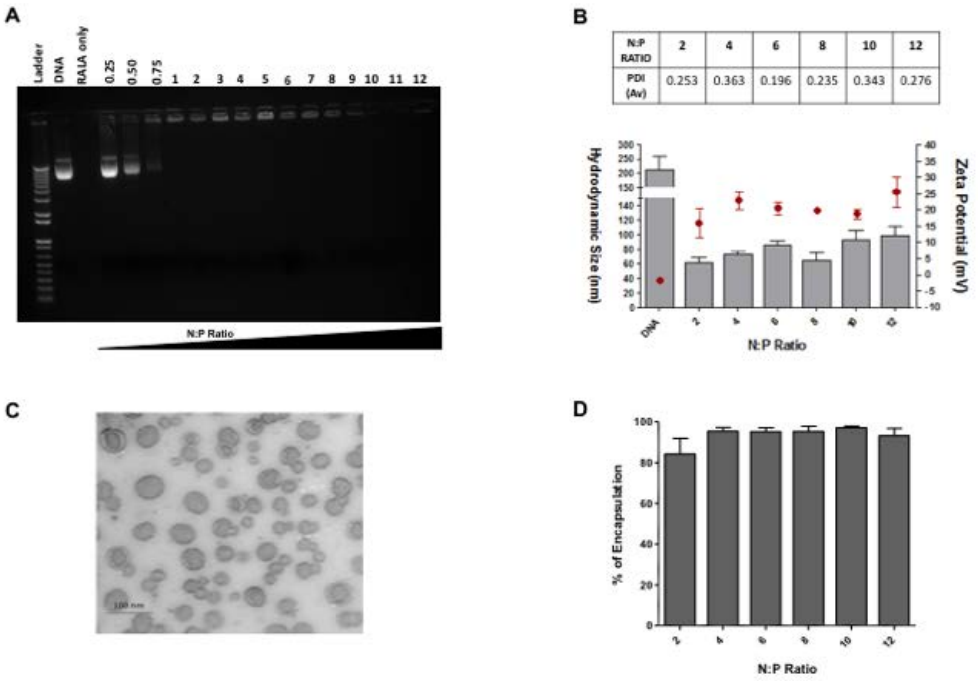
A
Ladder
DNA
RAIA only
0.25
0.50
0.75
1 2 3 4 5 6 7 8 9 10 11 12
N:P Ratio
B
N:P RATIO | 2 | 4 | 6 | 8 | 10 | 12
PDI (Av) | 0.253 | 0.363 | 0.196 | 0.235 | 0.343 | 0.276
Hydrodynamic Size (nm)
Zeta Potential (mV)
DNA
N:P Ratio
C
D
% of Encapsulation
N:P Ratio

Figure 2

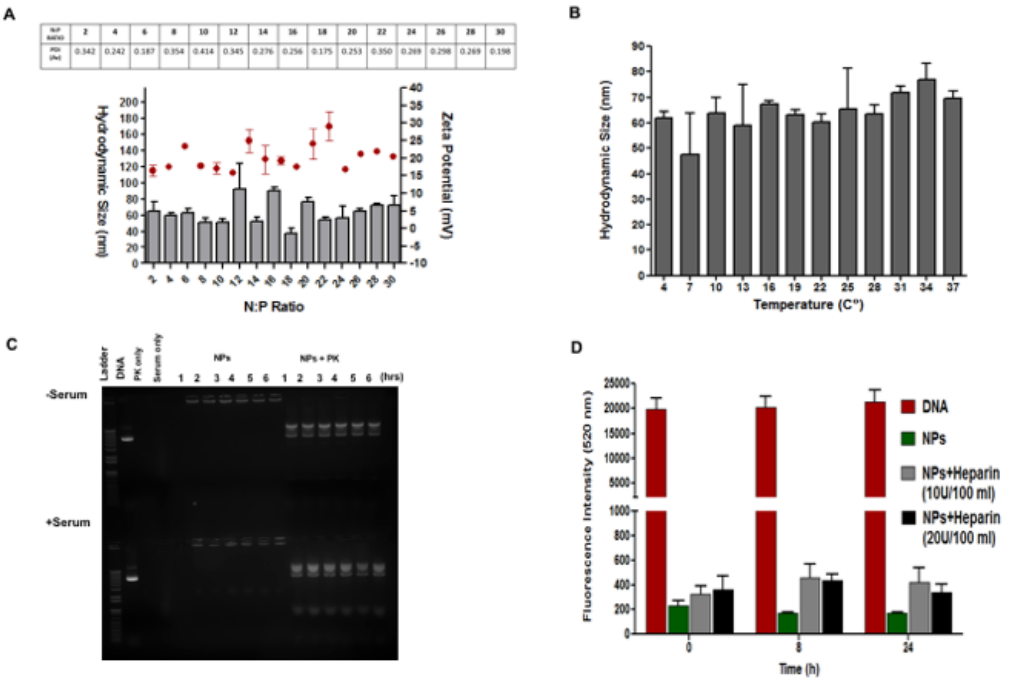
A
N:P Ratio
Hydrodynamic Size (nm)
Zeta Potential (mV)
B
Hydrodynamic Size (nm)
Temperature (C°)
C
Ladder
DNA
PK only
Serum only
NPs
NPs + PK
(hrs)
-Serum
+Serum
D
Fluorescence Intensity (520 nm)
Time (h)
DNA
NPs
NPs+Heparin (10U/100 ml)
NPs+Heparin (20U/100 ml)

Figure 3

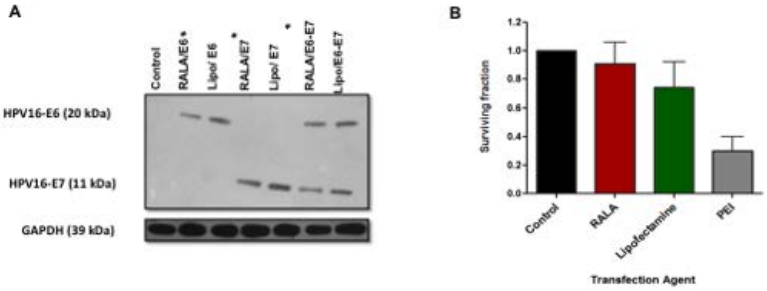
A
Control
RALA/E6+
Lipo/ E6
RALA/E7
Lipo/ E7
RALA/E6-E7
Lipo/E6-E7
HPV16-E6 (20 kDa)
HPV16-E7 (11 kDa)
GAPDH (39 kDa)
B
Surviving fraction
1.2
1.0
0.8
0.6
0.4
0.2
0.0
Control
RALA
Lipofectamine
PEI
Transfection Agent

Figure 4

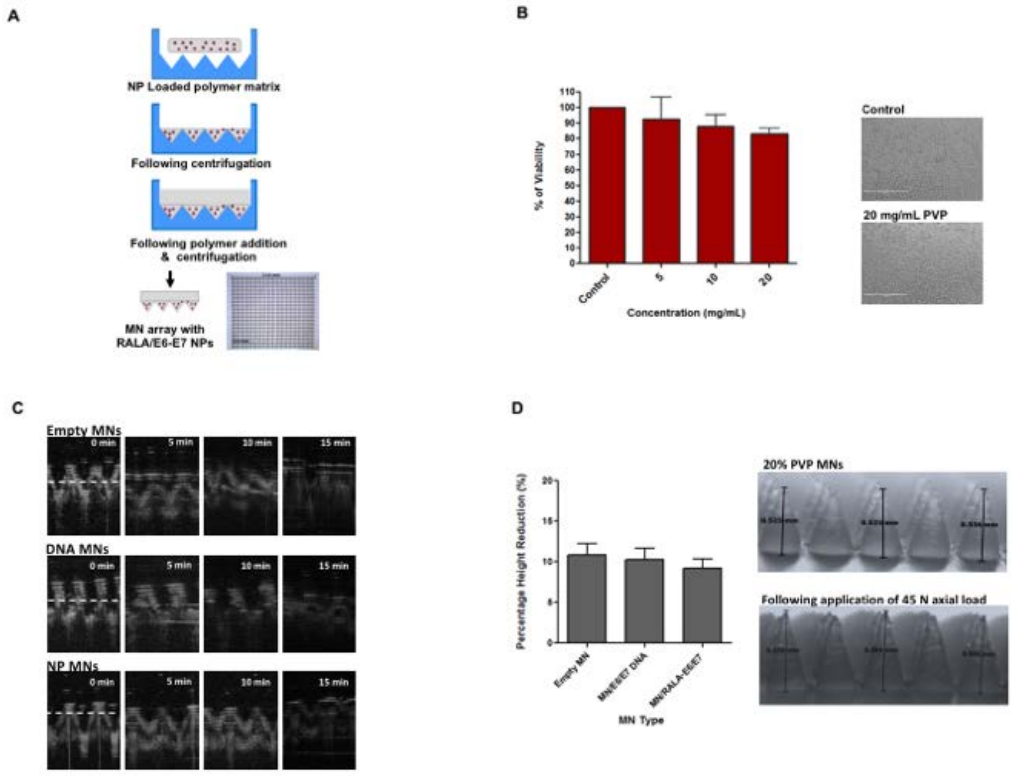
A
NP Loaded polymer matrix
Following centrifugation
Following polymer addition & centrifugation
MN array with RALA/E6-E7 NPs
B
% of Viability
Control
5
10
20
Concentration (mg/mL)
Control
20 mg/mL PVP
C
Empty MNs
DNA MNs
NP MNs
0 min
5 min
10 min
15 min
D
Percentage Height Reduction (%)
Empty MN
MN/E6/E7 DNA
MN/RALA-E6/E7
MN Type
20% PVP MNs
Following application of 45 N axial load

Figure 5

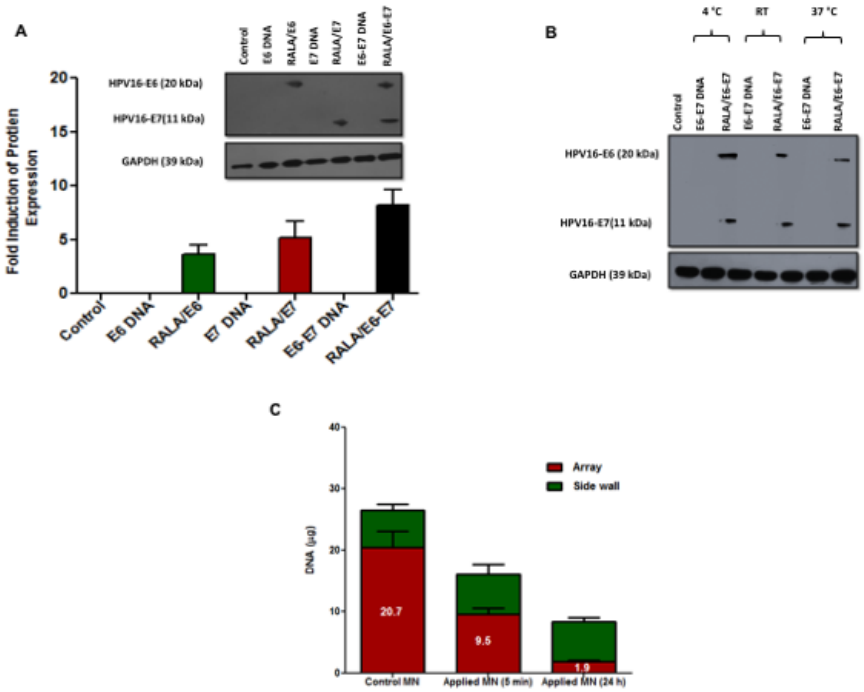
A
Control
E6 DNA
RALA/E6
E7 DNA
RALA/E7
E6-E7 DNA
RALA/E6-E7
HPV16-E6 (20 kDa)
HPV16-E7(11 kDa)
GAPDH (39 kDa)
Fold Induction of Protien Expression
20
15
10
5
0
Control
E6 DNA
RALA/E6
E7 DNA
RALA/E7
E6-E7 DNA
RALA/E6-E7
B
4 °C
RT
37 °C
Control
E6-E7 DNA
RALA/E6-E7
E6-E7 DNA
RALA/E6-E7
E6-E7 DNA
RALA/E6-E7
HPV16-E6 (20 kDa)
HPV16-E7(11 kDa)
GAPDH (39 kDa)
C
Array
Side wall
DNA (µg)
40
30
20
10
0
20.7
9.5
1.9
Control MN
Applied MN (5 min)
Applied MN (24 h)

Figure 6

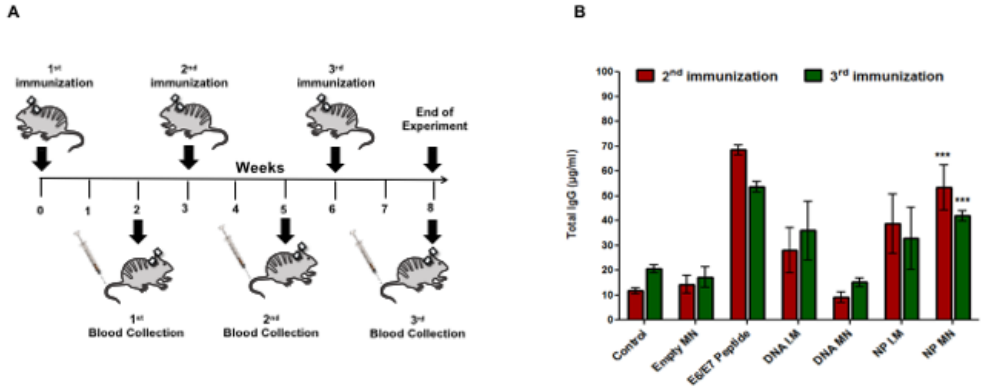
A
1st immunization
2nd immunization
3rd immunization
End of Experiment
Weeks
0
1
2
3
4
5
6
7
8
1st Blood Collection
2nd Blood Collection
3rd Blood Collection
B
2nd immunization
3rd immunization
Total IgG (µg/ml)
100
90
80
70
60
50
40
30
20
10
0
***
***
Control
Empty MN
E6/E7 Peptide
DNA LM
DNA MN
NP LM
NP MN

Figure 7

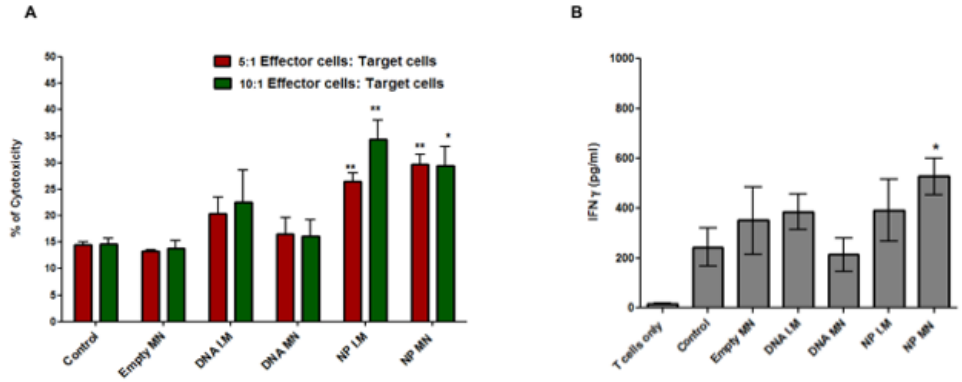
A
5:1 Effector cells: Target cells
10:1 Effector cells: Target cells
% of Cytotoxicity
Control
Empty MN
DNA LM
DNA MN
NP LM
NP MN
B
IFN γ (pg/ml)
T cells only
Control
Empty MN
DNA LM
DNA MN
NP LM
NP MN

Figure 8

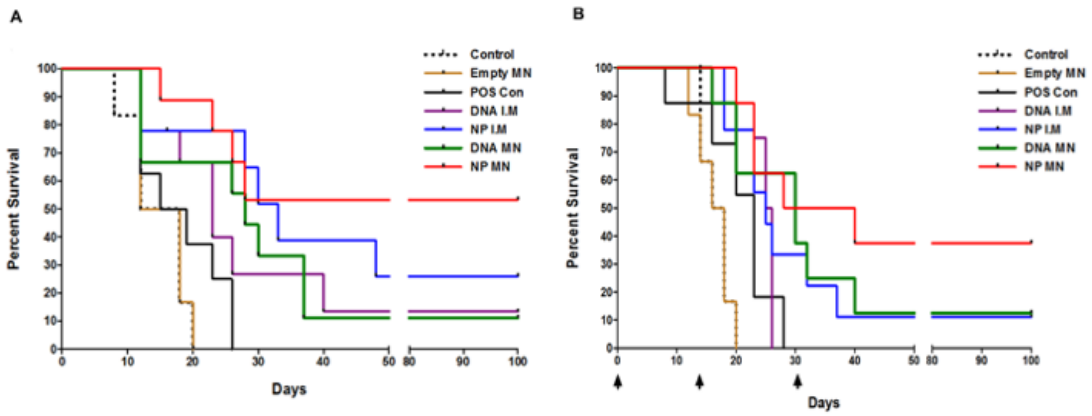
A
B
Percent Survival
Days
Control
Empty MN
POS Con
DNA I.M
NP I.M
DNA MN
NP MN